A Robust 3D Face Recognition Algorithm Using Passive Stereo Vision

Akihiro HAYASAKA[†a], *Nonmember*, Koichi ITO[†b], Takafumi AOKI[†], *Members*,
Hiroshi NAKAJIMA[††], *Nonmember, and* Koji KOBAYASHI[††], *Member*

SUMMARY The recognition performance of the conventional 3D face recognition algorithm using ICP (Iterative Closest Point) is degraded for the 3D face data with expression changes. Addressing this problem, we consider the use of the expression-invariant local regions of a face. We find the expression-invariant regions through the distance analysis between 3D face data with the neutral expression and smile, and propose a robust 3D face recognition algorithm using passive stereo vision. We demonstrate efficient recognition performance of the proposed algorithm compared with the conventional ICP-based algorithm through the experiment using a stereo face image database which includes the face images with expression changes.
key words: biometrics, face recognition, 3D face, facial expression, phase-only correlation

1. Introduction

With the needs for reliable human authentication in various applications such as access control, etc., biometric authentication has been receiving extensive attention over the past decade [1]. Among all the biometric techniques, face recognition has been an area of intense research [2].

Most of the reported approaches to automatic human face recognition use two-dimensional (2D) images. However, face recognition techniques using 2D images are affected strongly by variations in pose and illumination. The robust feature detection in 2D face images is still an open difficulty. On the other hand, recently, the use of three-dimensional (3D) information has gained much attention [3], [4], since 3D data is not affected by translation, rotation and scaling, and is immune to the effect of illumination variation. The 3D face recognition method acquires 3D facial information (facial structure) obtained from the 3D scanner and then identifies a person by calculating the similarity between facial structures.

The reported 3D face recognition systems have used active and passive 3D scanners to capture 3D facial structure. The active 3D scanners can capture accurate and dense 3D face data. However, the use of active 3D scanners is not necessarily desirable in many cases of human recognition applications, since the active 3D measurement

employs structured illumination (structure projection, phase shift, gray-code demodulation, etc.) or laser scanning. The passive 3D scanners based on stereo vision have the advantages of simplicity and applicability, since the passive 3D scanners require simple instrumentation. However, poor reconstruction quality still remains as a major issue for passive 3D measurement. Addressing this problem, Takita et al. [5] and Muquit et al. [6] have proposed sub-pixel correspondence search techniques for stereo vision to improve the reconstruction accuracy of the passive 3D scanners. In this paper, we employ the passive 3D scanner to capture 3D face data, since the passive scanner is applicable for anthropometric applications, and the local 3D data can be reconstructed based on the local region on the 2D stereo image.

In general, an ICP (Iterative Closest Point) algorithm [7], [8] is usually used to identify the 3D face data. The ICP algorithm aligns the location of 3D data sets by a rigid body transformation. For face images with the neutral expression, the ICP algorithm works well, while for face images with expression changes, the ICP algorithm does not work well. Addressing this problem, there are some works on the expression-invariant 3D face recognition algorithm [9]–[11]. Chang et al. [9] and Faltemire et al. [10] have proposed to use the nose region which is invariant to facial expressions. Lu et al. [11] have proposed the deformation modeling using TPS (Thin-Plate Spline) to deal with 3D surface movement due to expression changes.

In this paper, we analyze the local facial regions which are invariant to facial expression changes. According to the result of analysis, we propose a robust 3D face recognition algorithm using expression-invariant local regions of faces. Experimental evaluation demonstrates efficient recognition performance of the proposed algorithm compared with the conventional algorithm.

This paper is organized as follows: Sect. 2 presents 3D face data acquisition using our passive stereo vision system. Section 3 describes a robust 3D face recognition algorithm proposed in this paper. Section 4 presents a set of experiments for evaluating verification performance of the proposed algorithm. In Sect. 5, we end with some conclusions.

2. 3D Face Data Acquisition Using Passive Stereo Vision

We have developed the 3D facial capture system using passive stereo vision to capture high-quality 3D face data un-

(a)

(b)

Fig. 1 Passive 3D facial capture system: (a) system configuration and (b) close-up view of the camera head and system specification.
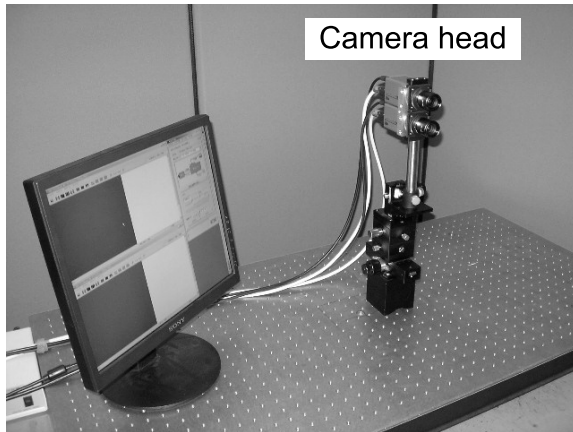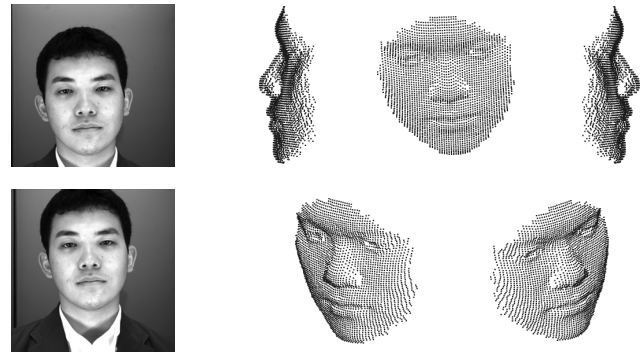
[Specifications]
- Camera: Adimec-1000m/D
  10 bits digital resolution
  monochrome
- Image size: 1000x1000 pixels
- Lens: μTRON, FV1520
  15 mm focal length
- Image grabber: Coreco Imaging
  X64-CL-DUAL-32M
- Measurement range: 400 ~ 600 mm
- Lighting: Ambient light

(a)   (b)

Fig. 2 Example of 3D face data captured by the passive 3D facial capture system: (a) stereo images captured by the system and (b) reconstructed 3D face data viewed from different angles.

der ambient lighting. Figure 1 shows the developed passive 3D measurement system. The system has one stereo camera head which consists of a pair of two parallel cameras. An important feature of the stereo camera head is that its baseline is designed as narrow as possible; the baseline is 46 mm limited simply by the size of the camera chassis. The narrow-baseline camera configuration makes it possible to find stereo correspondence automatically for every pixel, but a serious drawback is its low accuracy in the reconstructed 3D face data when compared with wide-baseline configuration. Addressing this problem, we employ a high-accuracy stereo correspondence technique using phase-based image matching proposed by Takita et al. [5] and Muquit et al. [6] to find accurate correspondences. Figure 2 shows an example of 3D face data captured by the developed system, which is automatically reconstructed. In this case, the number of reconstructed points is about 4,000. The accuracy of the developed system is evaluated through the experimental measurement of a reference planar object with wooden texture; the resulting RMS (Root Mean Square) error in measurement is 0.5 mm at a distance of 50 cm, which is comparable with the active 3D measurement system.

3. Robust 3D Face Recognition Algorithm

This section presents the proposed 3D face recognition algorithm which is robust against the facial expression. We first describe the conventional 3D face recognition algorithm using ICP. Next, we analyze the local facial regions which are invariant to facial expression changes. According to the result of analysis, we propose a robust 3D face recognition algorithm using expression-invariant local regions of faces.

3.1 Conventional 3D Face Recognition Algorithm

The major approaches for 3D face recognition acquire 3D face data using 3D scanners, align 3D facial structures using the ICP algorithm, and calculate the similarity based on some distance metrics [12], [13]. Lu et al. use the active 3D measurement system, i.e., a Minolta VIVID 910, to capture 3D face data [12], while Hayasaka et al. use the passive 3D measurement system using stereo vision [13]. Their experimental results show that the ICP algorithm works well for the 3D face data without changing facial expression. For 3D face images with expression changes, the ICP algorithm cannot be used, since the ICP algorithm is based on the rigid body transformation. Figure 3 shows a example of 3D face data with expression changes captured by the developed passive 3D measurement system. Two 3D face data shown in Fig. 3 are captured from the same person, but their facial structures are not the same due to the facial expression change. Thus, the 3D face data with expression changes are not accurately aligned using the ICP algorithm.

Addressing this problem, Chang et al. [9] matched multiple overlapped region around the nose and integrated matching results to make the final decision. Faltemire et al. [10] have used 28 local regions around the face and calculated the matching score using the Consensus Voting (CV) and Borda Count (BC) methods. Lu et al. [11] synthesized the deformation model learned from a small set of subjects and fitted the model to the input 3D face data to handle the 3D surface movement due to expression changes. Hayasaka

et al. [13] improved the ICP algorithm using the coarse-to-fine strategy and the nose region extraction. In this paper, we consider the use of local facial regions which are invariant to facial expression changes.

3.2 3D Face Data Analysis for Facial Expression Changes

We analyze the difference between 3D facial structures with expression changes. We align 3D face data with neutral ex-
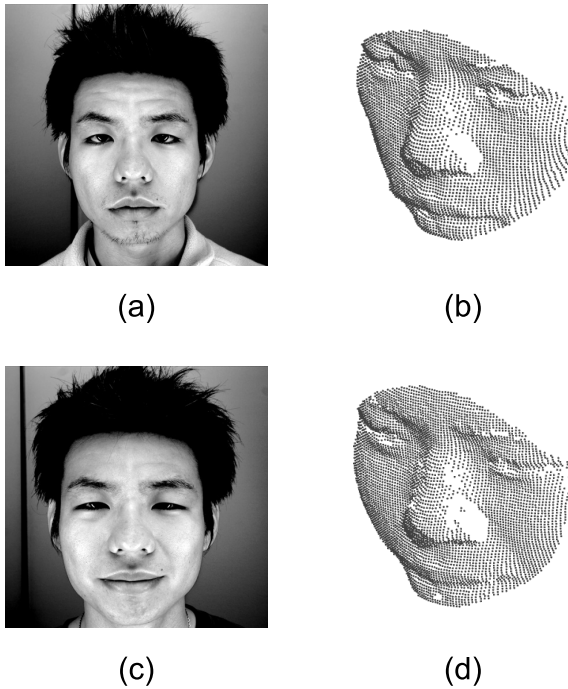

Fig. 3 Example of 3D face data with expression changes: (a) face image with neutral expression, (b) 3D face data with neutral expression, (c) face image with smile, and (d) 3D face data with smile.

pression and smile, which are captured from the same person, using the ICP algorithm and calculate the distance between aligned 3D face data. Figure 4 shows examples of the alignment result, i.e., the distance map, between 3D face data. If the distance equals to zero, the region indicates *gray*. As the distance increases, the color of the region is close to *black*. As shown in Fig. 4, the regions around cheek are *black* for all faces. Also, the regions around mouth are *black* for some faces. Other regions such as eyes and nose are *gray* for all faces. As a result, we expect that the use of 3D face data around eyes and nose makes it possible to achieve accurate 3D face recognition.

3.3 Local Region Extraction

This section describes the local region extraction for robust 3D face recognition. In general, it is time-consuming to extract the local regions around eyes and nose from the 3D face data. Chang et al. [9] proposed the local surface extraction method from 3D face data. This method is for the 3D surface data captured by active 3D measurement. At first, the 3D surface data is captured by the active 3D measurement system such as Minolta VIVID. Next, after calculating the surface curvature at each point on a 3D surface, the eye cavities and nose tip are detected based on the curvature type. And then, the local 3D surface centered at the nose tip is extracted. On the other hand, in the case of using stereo vision to capture 3D face data, the local 3D data can be reconstructed from the local region on the 2D stereo image. Thus, we extract the expression-invariant local region on the 2D image and reconstruct the local 3D data according to the extracted region. This results in reduction of computation time to obtain local 3D facial data. In this paper, we employ the feature points such as end points of eyes, mouth, etc. as landmark points to extract the local regions. The local 3D data extraction is performed as follows: (i) extract
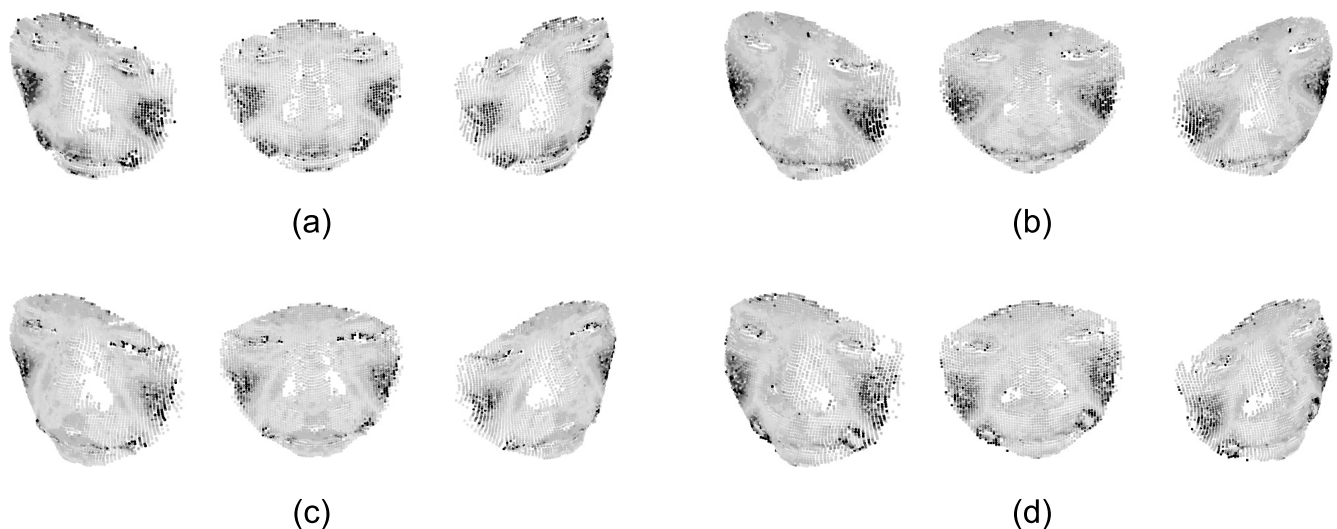

Fig. 4 Distance maps between 3D face data with neutral expression and smile, where *gray* indicates short distance and *black* indicates long distance: (a) Person A, (b) Person B, (c) Person C and (d) Person D.
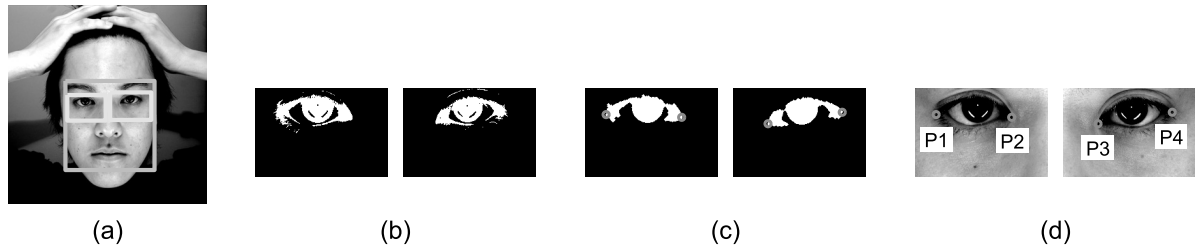
Fig. 5 End point extraction of eyes: (a) detection results of the whole face and eyes, (b) binary image of eye regions, (c) binary image after applying the morphological filter and end points and (d) extracted end points on the eye regions.
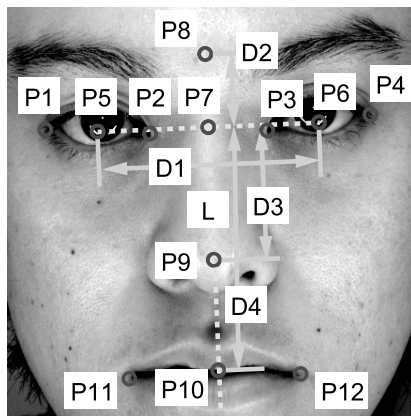

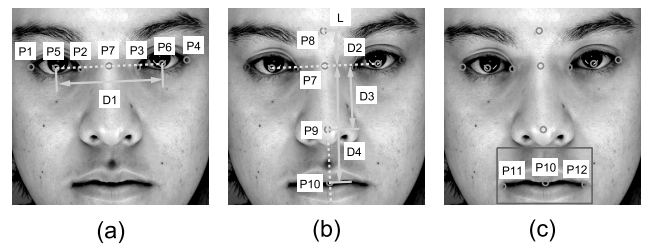**Fig. 6** Anthropometric face model and feature points on a face.

Fig. 7 Facial feature point extraction based on the anthropometric face model: (a) the right eye center, the left eye center and the midpoint of eyes, (b) the midpoint of eyebrows, the nose tip and the mouth center, and (c) the end points of the mouth.

both end points of eyes on the 2D stereo image, (ii) extract the feature points based on the anthropometric face model [14], (iii) extract the expression-invariant local region based on the feature points and (iv) reconstruct the local 3D data from the extracted local region on the 2D stereo image.

The following is the detailed procedure of end point extraction of eyes.

[End point extraction of eyes]

Step 1: Detect the whole face region using AdaBoost [15].

Step 2: Detect the eye regions from the upper part of the extracted face region using AdaBoost. Figure 5(a) shows detection results of the whole face region and eye regions.

Step 3: Convert the eye regions into the binary images by thresholding after enhancing the contrast as shown in Fig. 5(b).

Step 4: Apply the morphological filters to the binary images to reduce the noise effect.

Step 5: Extract both end points of eyes as both end points of the remaining regions, which indicate $P1$, $P2$, $P3$ and $P4$, as shown in Figs. 5(c) and (d).

According to the end points of eyes, we can estimate other feature points on nose, mouth, etc. using the anthropometric face model. In this paper, we employ the anthropometric face model proposed by Sohail et al. [14] as shown in Fig. 6. Finally, we get 12 feature points on the face. The following is the detailed procedure.

[Feature point extraction]

Step 1: Detect $P5$ and $P6$ as the right eye center and the

left eye center, respectively, and $P7$ as the midpoint of eyes between $P5$ and $P6$. Calculate the distance $D1$ between $P5$ and $P6$ as shown in Fig. 7(a).

Step 2: Obtain L as the perpendicular bisector of the line segment between $P5$ and $P6$. Detect $P8$ as the midpoint of eyebrows, which distance from $P7$ is $D2$. In the same way, detect $P9$ as the nose tip which distance from $P7$ is $D3$ and $P10$ as the mouth center which distance from $P7$ is $D4$. Note that the distance $D2$, $D3$ and $D4$ are defined as follows:

$$D2 = 0.33 \times D1, \quad D3 = 0.60 \times D1, \quad D4 = 1.10 \times D1,$$

where $P8$ is above $P7$, and $P9$ and $P10$ are below $P7$ as shown in Fig. 7(c).

Step 3: Detect both end points of the mouth from the region around $P10$ using the same procedure for the end point detection of eyes as shown in Fig. 7(c).

Based on the 12 extracted feature points, we define the 9 regions to be reconstructed for the succeeding recognition step: (i) the circular region including all feature points, (ii) the right eye region including only feature points on right eye ($D1 \times D2$ pixels), (iii) the left eye region including only feature points on left eye ($D1 \times D2$ pixels), (iv) the nose region including only feature points on nose ($3/4 \cdot D1 \times (D2 + (D3 + D4)/2)$ pixels), (v) the mouth region including only feature points on mouth ($5/4 \cdot D1 \times (D4 - D3)$ pixels), (vi) the eyes region including feature points on left and right eyes ($2 \cdot D1 \times D2$ pixels), (vii) the nose and mouth region including feature points on nose and mouth, (viii) the eyes and nose region including feature points on eyes and nose, and (ix) the eyes, nose and mouth region including feature points on eyes, nose and mouth. Note that we em-
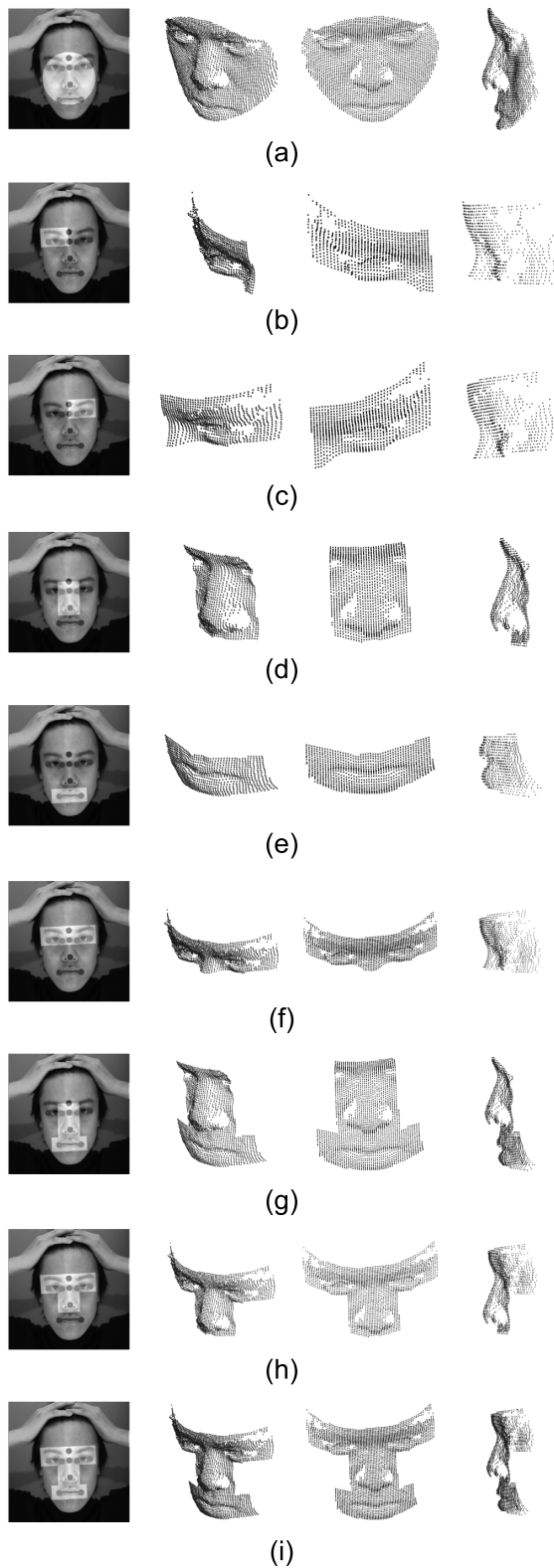
Fig. 8 Examples of the local face region and its 3D data: (a) whole face, (b) right eye, (c) left eye, (d) nose, (e) mouth, (f) eyes, (g) nose and mouth, (h) eyes and nose, (i) eyes, nose and mouth.
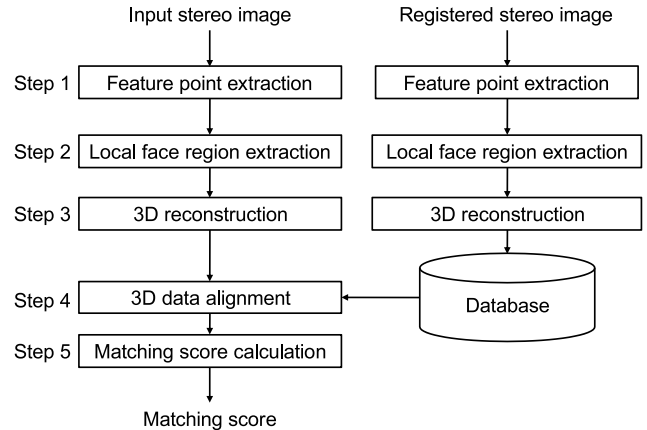

Fig. 9 Flow diagram of the proposed algorithm.

pirically decide the size of local regions. Figure 8 shows examples of the local face region used in this paper. We expect that the region (iv) is the most invariant region to the facial expression changes, since this region dose not include the cheek and mouth which structures depend on the facial expression changes. The region (viii) except for region on eye is also invariant to the facial expression changes, since the region having short distance on the distance map spread like "T," which includes regions around eyes and nose.

3.4 Proposed 3D Face Recognition Algorithm

This section presents a 3D face recognition algorithm proposed in this paper. The proposed algorithm consists of 5 steps: (i) feature point extraction, (ii) local face region extraction, (iii) 3D reconstruction, (iv) 3D data alignment, and (v) matching score calculation as shown in Fig. 9. In steps 4 and 5, we employ the modified ICP algorithm and score calculation method proposed in [13].

Step 1: Detect the end points of the eyes from the upper or lower camera image using **[end point extraction of eyes]**. Detect the 12 feature points on the face using **[feature point extraction]**.

Step 2: Extract the local face region based on the extracted feature points.

Step 3: Reconstruct the 3D data of the extracted local face region using the POC-based passive 3D measurement algorithm [5], [6].

Step 4: Align the input 3D data and the registered 3D data using the ICP algorithm.

Step 5: Calculate the distance, i.e., the dissimilarity, between the aligned 3D data as a matching score.

The following is the detailed procedure of Step 4. Let M be the set of 3D points of a face, and M' be the set of 3D points of another face. We find the closest point m'_i from M' as a corresponding point for every point m_i in M. Based on the current correspondence, we calculate the optimal transformation (i.e., rotation $\boldsymbol{R}$ and translation $\boldsymbol{t}$) between the two data sets M and M' using the least-square method. We transform the points in M' with $\boldsymbol{R}$ and $\boldsymbol{t}$. The above procedures

are repeated until convergence. To accelerate the computation, we adopt the coarse-to-fine strategy in the above ICP procedure, where the initial alignment starts with fewer corresponding points (1/32 of the total points) and the number of corresponding points gradually increases as the iteration step increases.

The following is the detailed procedure for matching score calculation. Dissimilarity between the two 3D facial data M and M' is evaluated by a simple point-to-plane distance [13]. For every point m_i in M, we first find the three points in M' that are closest to m_i. Then, we evaluate the distance d_i between the point m_i and the triangular patch formed by the three points. If the orthogonal projection of m_i onto the plane of the three points is not inside the triangular patch, we omit the point m_i for distance calculation, since m_i is not overlapped on the nearest triangular patch in M', that is, there is no point in M' corresponding to m_i. The distance between the two facial data is defined as an average of individual point-to-plane distances d_i.

4. Experiments and Discussion

This section describes a set of experiments using our face image databases for evaluating recognition performance of the proposed algorithm. The following experiments are carried out for the two databases.

- DB1
  This database consists of 192 stereo images with 24 subjects and 8 different stereo images of each face. The face images are captured under different conditions: one of them is with the closed eyes, two are with smile, and others are with the neutral expression. Figure 10 shows the examples of the face image and their 3D data in this database.
- DB2
  This database consists of 300 stereo images with 15 subjects and 20 different stereo images (5 expression × 4 times) of each face. The captured face images have different expression: neutral, smile, anger, surprise and sadness. The facial expression changes in this database are larger than those in DB1. Figure 11 shows the examples of the face image and their 3D data in this database.

The performance of the biometrics-based verification system is evaluated by the Receiver Operating Characteristic (ROC) curve, which illustrates the False Non-Match Rate (FNMR) against the False Match Rate (FMR) at different thresholds on the matching score. We first evaluate the FNMR for all the possible combinations of genuine attempts; the number of attempts is $_8C_2 \times 24 = 672$ for DB1 and $_{20}C_2 \times 15 = 2,850$ for DB2, respectively. Next, we evaluate the FMR for all the possible combinations of impostor attempts; $_{192}C_2 - 672 = 17,664$ for DB1 and $_{300}C_2 - 2,850 = 42,000$ for DB2, respectively. The performance is also evaluated by the Equal Error Rate (EER), which is defined as the error rate where the FNMR and the FMR are equal.

(a)   (b)   (c)

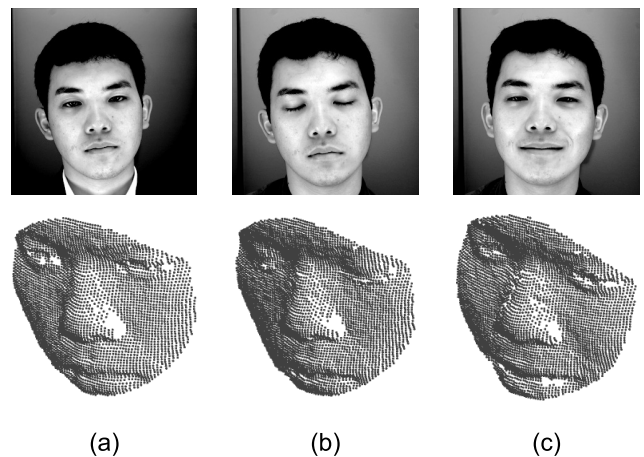**Fig. 10**   Examples of the face image and 3D face data in DB1: the face with (a) neutral expression, (b) closed eyes and (c) smile.

(a)   (b)   (c)   (d)   (e)
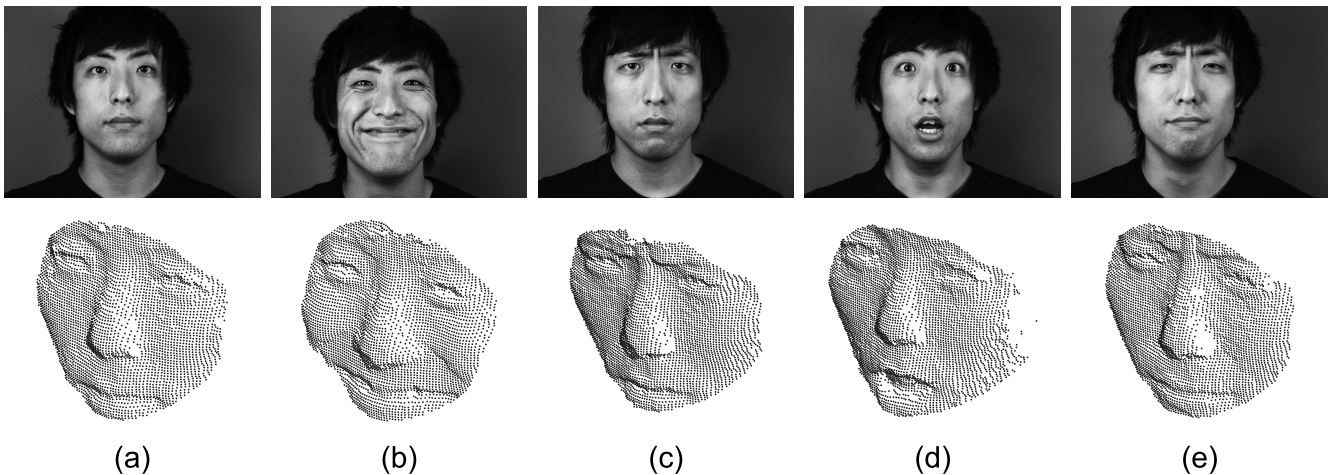
Fig. 11   Examples of the face image and 3D face data in DB2: the face with (a) neutral expression, (b) smile, (c) anger, (d) surprise and (e) sadness.
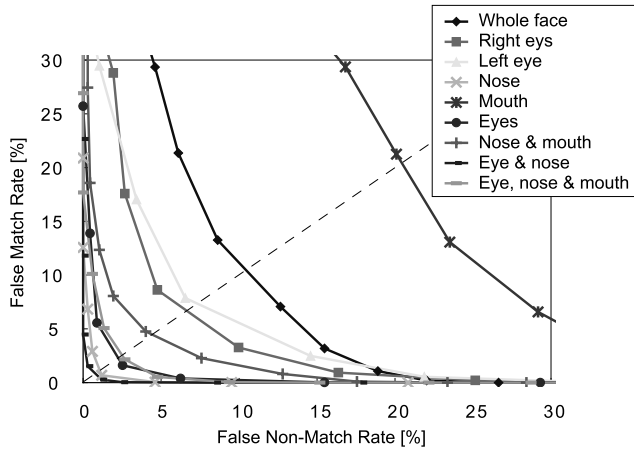
Fig. 12   ROC curves for each face region (DB1).

Fig. 13   ROC curves for each face region (DB2).

Table 1   EERs for each face region (DB1).

	Face region	EER [%]
(i)	Whole face	10.433
(ii)	Right eye	6.356
(iii)	Left eye	7.292
(iv)	Nose	1.020
(v)	Mouth	20.274
(vi)	Eyes	2.015
(vii)	Nose and mouth	4.315
(viii)	Eyes and nose	0.531
(ix)	Eyes, nose and mouth	2.465

Table 2   EERs for each face region (DB2).

	Face region	EER [%]
(i)	Whole face	20.089
(ii)	Right eye	21.071
(iii)	Left eye	19.658
(iv)	Nose	8.064
(v)	Mouth	33.943
(vi)	Eyes	15.743
(vii)	Nose and mouth	21.721
(viii)	Eyes and nose	9.883
(ix)	Eyes, nose and mouth	16.046

We compare recognition performance among the proposed algorithm using 9 different 3D face data which are reconstructed from (i) the whole face region, (ii) the right eye region, (iii) the left eye region, (iv) the nose region, (v) the mouth region, (vi) the eyes region, (vii) the nose and mouth region, (viii) the eyes and nose region and (ix) the eyes, nose and mouth region. The condition of (i) is almost the same as the conventional ICP-based algorithm [12], [13].

As for DB1, Fig. 12 and Table 1 show the ROC curves and the EERs for each face region, respectively. Compared with the whole face region (i) and eyes, nose and mouth region (ix), EER of (i) is higher than that of (ix). From the results of eyes and nose region (viii) and eyes, nose and mouth region (ix), the facial region around mouth is not effective to recognize a human face. These facts indicate that the structures around cheek and mouth vary depending on the facial expressions. On the other hand, the facial structure around eyes and nose is invariant to facial expression changes, since the eyes and nose region (viii) exhibits the highest performance compared with other regions.

As for DB2, Fig. 13 and Table 2 show the ROC curves and the EERs for each face region, respectively. The recognition accuracy for DB2 is decreased compared with that for DB1, since the facial expression changes in DB2 are larger than those in DB1. The trend of recognition performance for each local regions of face images in DB2 is similar to that in DB1. That is, the use of facial structure around nose exhibits higher recognition performance compared with other
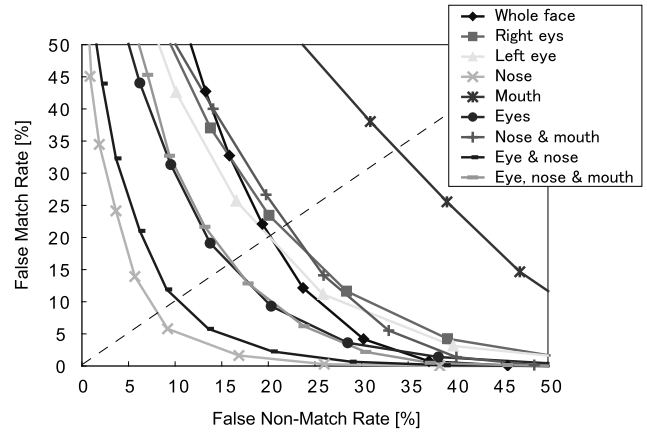
local facial structures. Table 3 shows the EERs for each facial expression change. As a result, the local facial structure around nose exhibits the most stable recognition performance compared with other local facial structures. This indicates that the 3D facial structure around nose varies a little, even if the facial expression changes are large.

The computation time of the proposed algorithm is evaluated by using MATLAB 6.5.1 on Core2 Extreme X9650 3.00 GHz. The computation times for 3D face reconstruction and 3D face matching of whole face are 12.24 sec. and 5.03 sec., respectively. The total computation time for whole face is 17.26 sec. On the other hand, the computation times for 3D face reconstruction and 3D face matching for nose region are 9.99 sec. and 0.55 sec., respectively. The total computation time for nose region is 10.53 sec. Thus, the use of local facial region makes possible to reduce the computation time and to improve the matching accuracy of 3D face recognition.

As is observed in the above experiments, the use of local facial region around eyes and nose is effective for accurate 3D face recognition.

5. Conclusion

This paper has proposed the robust 3D face recognition algorithm using expression-invariant local regions. Through the distance analysis between 3D face data with the neutral expression and smile, the local regions around eyes and nose are found as the expression-invariant regions. We demon-

Table 3　EERs [%] for each facial expression change (DB2).

	Whole face	Right eye	Left eye	Nose	Mouth	Eyes	Nose and mouth	Eyes and nose	Eyes, nose and mouth
All data	20.09	21.07	19.66	8.06	33.94	15.74	21.72	9.88	16.05
Neutral	0.00	7.53	4.44	0.00	4.58	2.98	0.00	0.00	0.00
Smile	6.67	11.33	7.78	2.74	16.67	4.44	4.44	2.22	4.44
Anger	3.33	15.56	14.44	3.33	15.56	11.11	6.67	5.56	5.56
Surprise	5.56	16.77	15.56	3.11	23.27	8.89	11.11	3.33	3.62
Sadness	3.33	13.55	9.39	1.98	14.44	5.66	7.78	3.33	5.56

strate efficient performance of the proposed algorithm compared with the conventional algorithm through the experiment using the stereo face images with expression changes.

References

[1] A.K. Jain, P. Flynn, and A.A. Ross, Handbook of Biometrics, Springer, 2007.

[2] S.Z. Li and A.K. Jain, Handbook of Face Recognition, Springer, 2005.

[3] A. Scheenstra, A. Ruifrok, and R. Veltkamp, "A survey of 3D face recognition methods," Audio- and Video-Based Biometric Person Authentication (AVBPA 2005), vol.3546, pp.891–899, July 2005.

[4] K.W. Bowyer, K. Chang, and P. Flynn, "A survey of 3D and multimodal 3D+2D face recognition," Notre Dame Department of Computer Science and Engineering Technical Report, Jan. 2004.

[5] K. Takita, M.A. Muquit, T. Aoki, and T. Higuchi, "A sub-pixel correspondence search technique for computer vision applications," IEICE Trans. Fundamentals, vol.E87-A, no.8, pp.1913–1923, Aug. 2004.

[6] M.A. Muquit, T. Shibahara, and T. Aoki, "A high-accuracy passive 3D measurement system using phase-based image matching," IEICE Trans. Fundamentals, vol.E89-A, no.3, pp.686–697, March 2006.

[7] P.J. Besl and N.D. McKay, "A method for registration of 3-D shapes," IEEE Trans. Pattern. Anal. Mach. Intell., vol.14, no.2, pp.239–256, Feb. 1992.

[8] Z. Zhang, "Iterative point matching for registration of free-form curves," Technical Report RR-1658, INRIA-Sophia Antipolis, Valbonne Cedex, France, 1992.

[9] K.I. Chang, K.W. Bowyer, and P.J. Flynn, "Multiple nose region matching for 3D face recognition under varying facial expression," IEEE Trans. Pattern. Anal. Mach. Intell., vol.28, no.10, pp.1695–1700, Oct. 2006.

[10] T.C. Faltemier, K.W. Bowyer, and P.J. Flynn, "A region ensemble for 3-D face recognition," IEEE Trans. Information Forensics and Security, vol.3, no.1, pp.62–73, March 2008.

[11] X. Lu and A.K. Jain, "Deformation modeling for robust 3D face matching," IEEE Trans. Pattern. Anal. Mach. Intell., vol.30, no.8, pp.1346–1356, Aug. 2008.

[12] X. Lu, D. Colbry, and A.K. Jain, "Three-dimensional model based face recognition," Proc. Int. Conf. Pattern Recognition, vol.I, pp.362–366, Aug. 2004.

[13] A. Hayasaka, T. Shibahara, K. Ito, T. Aoki, H. Nakajima, and K. Kobayashi, "A passive 3D face recognition system and its performance evaluation," IEICE Trans. Fundamentals, vol.E91-A, no.8, pp.1974–1981, Aug. 2008.

[14] A.S.M. Sohail and P. Bhattacharya, "Detection of facial feature points using anthropometric face model," Proc. IEEE Int. Conf. Signal-Image Technology & Internet-Based Systems, pp.656–665, Dec. 2006.

[15] P. Viola and M. Jones, "Robust real time object detection," Proc. 2nd Int. Workshop on Statistical and Computational Theories of Vision–Modeling, Learning, Computing and Sampling, pp.1–25, July 2001.

Akihiro Hayasaka　received the B.E. degree in information engineering, and the M.S. degree in information sciences from Tohoku University, Sendai, Japan, in 2004 and 2006, respectively. He is currently working toward the Ph.D. degree. His research interest includes signal and image processing, and biometric authentication.

Koichi Ito　received the B.E. degree in electronic engineering, and the M.S. and Ph.D. degrees in information sciences from Tohoku University, Sendai, Japan, in 2000, 2002 and 2005, respectively. He is currently an Assistant Professor of the Graduate School of Information Sciences at Tohoku University. From 2004 to 2005, he was a Research Fellow of the Japan Society for the Promotion of Science. His research interest includes signal and image processing, and biometric authentication.

Takafumi Aoki　received the B.E., M.E., and D.E. degrees in electronic engineering from Tohoku University, Sendai, Japan, in 1988, 1990, and 1992, respectively. He is currently a Professor of the Graduate School of Information Sciences at Tohoku University. For 1997–1999, he also joined the PRESTO project, Japan Science and Technology Corporation (JST). His research interests include theoretical aspects of computation, VLSI computing structures for signal and image processing, multiple-valued logic, and biomolecular computing. Dr. Aoki received the Outstanding Paper Award at the 1990, 2000, 2001 and 2006 IEEE International Symposiums on Multiple-Valued Logic, the Outstanding Transactions Paper Award from the Institute of Electronics, Information and Communication Engineers (IEICE) of Japan in 1989 and 1997, the IEE Ambrose Fleming Premium Award in 1994, the IEICE Inose Award in 1997, the IEE Mountbatten Premium Award in 1999, the Best Paper Award at the 1999 IEEE International Symposium on Intelligent Signal Processing and Communication Systems, the IP Award at the 7th LSI IP Design Award in 2005, and the Best Paper Award at the 14th Workshop on Synthesis And System Integration of Mixed Information technologies.

Hiroshi Nakajima   received the B.E. degree in electronic engineering from Tohoku University, Sendai, Japan, in 1990. He is currently with Systems Development Department, Yamatake Corporation, Fujisawa, Japan. His research interest includes biometric image processing.

Koji Kobayashi   received the B.E. and M.E. degrees in electronic engineering from Tohoku University, Sendai, Japan, in 1976, and 1978, respectively. He is currently a general manager of Vision Sensing Department, Yamatake Corporation, Fujisama, Japan. His general interests includes real-time automation system architecture, network communication protocol LSI, biometric image processing, CMOS image sensor, and three-dimensional sensing.